THE JOURNAL OF PHYSICAL CHEMISTRY A

 VOLUME 108, NUMBER 2, JANUARY 15, 2004

ARTICLES

Photochemistry of Diiodomethane in Solution Studied by Femtosecond and Nanosecond Laser Photolysis. Formation and Dark Reactions of the CH_2I-I Isomer Photoproduct and Its Role in Cyclopropanation of Olefins

Alexander N. Tarnovsky,*,† Villy Sundström, Eva Åkesson,* and Torbjörn Pascher

Contribution from the Department of Chemical Physics, Lund University, Box 124, 221 00 Lund, Sweden

Received: May 21, 2003; In Final Form: October 16, 2003

Femtosecond and nanosecond photolysis of CH_2I_2 in acetonitrile at an excitation wavelength of 266-nm yield the ground-state CH_2I-I isomer product in ~70% quantum yield. High isomer formation quantum yields (>70%) were measured also in *n*-hexane, dichloromethane, methanol, and ethanol using nanosecond photolysis. The CH_2I-I product is formed biphasically within ~15 ps after excitation and can survive on a nanosecond to microsecond time scale before it decays via a mixture of first- and second-order processes. At 21 °C, the first-order rate constants are 1.8×10^5 s^{-1} in *n*-hexane, with the measured apparent activation energy of 41 ± 2 kJ mol^{-1} (5−55 °C), and 4.3×10^6 s^{-1} in acetonitrile. These rate constants correspond to intramolecular decomposition of CH_2I-I into a $CH_2I^{\bullet}$ radical and an I atom, with the additional formation of I^- in acetonitrile. In methanol and ethanol, the CH_2I-I isomer decays faster with the pseudo-first-order rate constants of 2.0×10^8 and 1.3×10^8 s^{-1}, respectively, and as in acetonitrile, I_3^- and I_2^- ion products dominate the absorption of photolyzed CH_2I_2 samples at long times. The thermodynamics of the CH_2I_2 system and its implication for the CH_2I-I formation mechanism are discussed. A possible role of the CH_2I-I isomer as a methylene transfer agent in photocyclopronation of olefins is investigated. Vibrationally relaxed CH_2I-I is demonstrated to react with cyclohexene yielding an I_2 leaving group with the second-order rate constants ~4.4×10^5 M^{-1} s^{-1} in *n*-hexane, 3.4×10^6 M^{-1} s^{-1} in dichloromethane, and 4.2×10^6 M^{-1} s^{-1} in acetonitrile.

1. Introduction

In the ultrafast transient absorption study on photodissociation of diiodomethane (CH_2I_2) performed in this laboratory to obtain a deeper microscopic understanding of the "solvent cage effect",[1] the interesting CH_2I-I isomer photoproduct has been observed on the picosecond time scale.[2] Here, we examine the photochemical reactions in CH_2I_2 solutions on a much longer time scale—up to milliseconds. The photochemistry of CH_2I_2 has been the subject of extensive studies over the years due to interest in fragmentation dynamics and reaction control.[3−12] Excitation of gas-phase CH_2I_2 with a low-energy UV photon ($h\nu$ < 5 eV) populates a repulsive state(s),[3,4,8] and it is agreed that at least five excited electronic states are involved in the region 200−370 nm.[3,8,13] In the dissociation process, the initially activated I−C−I symmetric stretch of CH_2I_2 is coupled to I−C−I

* To whom correspondence should be addressed. E-mail: Alexander.Tarnovsky@psi.ch (A.N.T.); Eva.Akesson@chemphys.lu.se (E.Å.).

† Present address: Laboratory of Condensed Phase Ultrafast Spectroscopy (LCPUS), Institute of Molecular and Biological Chemistry, EPFL, Lausanne, CH-1015 Lausanne, Switzerland.

10.1021/jp035406n CCC: $27.50
Published on Web 12/16/2003

asymmetric stretch leading to breaking of one of the two C−I bonds[8,11]

$$CH_2I_2 \xrightarrow{h\nu} CH_2I_2^* \rightarrow CH_2I^{\bullet} + I^{\bullet}\ (^2P_{3/2} \text{ or } ^2P_{1/2}) \qquad (1)$$

and the $CH_2I^{\bullet}$ fragment is formed with a high degree of internal excitation.[4,5] Studies of UV photochemistry of CH_2I_2 in the condensed phase agree that homolytic cleavage of the C−I bond occurs initially,[2,14−16] yet different accounts have been presented for the ensuing chemistry. In polar solvents, it has been proposed that the primary radicals undergo electron transfer within the solvent cage to afford an ion pair[14] (for 1,*n*-diiodoalkanes in general, as reviewed[17]). High yield cyclopropanation of a wide variety of olefins in the presence of CH_2I_2 irradiated by UV light has been reported.[18−20] The high degree of electrophilic selectivity of the diiodomethane photocyclopropanation reaction and the lack of appreciable C−H insertion indicate that the reactive species is not a free carbene. The methylene transfer agent has been postulated to be the α-iodo-cation (CH_2I^+) formed as the ion pair undergoes loss of iodide.[14,20] Photoexcitation,[16,21,22] direct photoionization,[23] and radiolysis[24,25] of CH_2I_2 in a variety of condensed-phase environments all give rise to two absorption bands peaking in the UV (∼370−390 nm, strong) and visible (∼530−570 nm, weak) regions, which have been proposed to be due to trapped electrons,[21] $CH_2I^{\bullet}$ (visible band),[22] and $CH_2I_2^+$ (UV band[22,24] and both bands[16,23,25]). Maier and co-workers observed similar absorption bands for cold (12 K) argon and nitrogen matrices and polyethylene films all containing CH_2I_2 irradiated at a photon energy insufficient for ion production, and convincingly assigned these bands to the isomer of diiodomethane (isodiiodomethane, CH_2I-I).[26,27] In the suggested mechanism, photoexcitation of CH_2I_2 yields the iodomethyl−iodine radical pair, which collapses either to the parent or to the isomer (equilibrium ratio 70:30 for optimized conditions for photolysis). UV/vis and IR absorption of the isomer did not fade unless the temperature of a polyethylene film was above 100 K, indicating a bonding interaction between the iodine atoms.[26,27] Recent ab initio calculations have predicted that the I−I bond in isolated CH_2I-I is weak.[28−31]

The photodissociation dynamics of CH_2I_2 in room temperature solvents have been investigated using ultrafast pump−probe[2,15,16] and transient resonance Raman (TRR) spectroscopy.[32−34] Transient absorption spectra following 310-nm excitation of CH_2I_2 in acetonitrile reveal that the excited molecule rapidly dissociates into $CH_2I^{\bullet}$ and $I^{\bullet}$ fragments, which recombine on a picosecond time scale to form the CH_2I-I product that absorbs in two bands at ∼390 and ∼560 nm.[2] This interpretation differs from those of earlier pump−probe studies. Specifically, (1) 620-nm transient absorbance for 310-nm excitation of CH_2I_2 in chlorinated solvents was ascribed to $CH_2I^{\bullet}$ undergoing geminate recombination into the parent molecule: the concept of primary geminate recombination of polyatomic radicals controlled by a single collision with the solvent cage was put forward;[15] (2) the product 390-nm band produced in acetonitrile solution of CH_2I_2 using a 268-nm excitation was ascribed to $CH_2I_2^+$.[16] The TRR experiments in conjunction with density functional theory (DFT) calculations by Phillips and co-workers have confirmed that CH_2I-I is formed upon UV excitation of CH_2I_2 in cyclohexane and acetonitrile. They also showed that CH_2I-I is responsible for the product ∼390 nm absorption band[32,33] and suggested the contribution of both CH_2I-I and $CH_2I_2^+$ to the ∼560 nm band.[34] Recently, the same group has proposed CH_2I-I as a methylene transfer agent in the photocyclopropanation reactions of olefins that use CH_2I_2 as a reagent on the basis of DFT calculations of gas-phase reaction routes between olefin (ethylene) and vibrationally cold probable products of CH_2I_2 photolysis. CH_2I-I was calculated to react with ethylene via a transition state at ∼12−14 kJ mol^{-1} above the reactants, whereas $CH_2I^{\bullet}$ and CH_2I^+ were found to react via more difficult reaction routes.[30,31] Nanosecond TRR experiments on concentrated CH_2I_2 samples (0.24 M) in neat olefin (cyclohexene) showed the disappearance of the CH_2I-I isomer and development of a I_2:cyclohexene complex within 5−10 ns after the 266-nm laser pulse (pulse width ∼4 ns).[35] This was interpreted as a fast reaction between CH_2I-I and cyclohexene leading to a photocyclopropanated product and I_2.[35] This is rather controversial as, first, some secondary chemistry may have been involved (cf. the CH_2I-I decay was quenched, being slower only by a factor of 2 in the more viscous reference solvent cyclohexane). Second, vibrationally hot photoproducts, e.g., $CH_2I^{\bullet}$, could react with cyclohexene neighbors (cf. the amount of CH_2I-I produced by the laser pulse was smaller in cyclohexene than in cyclohexane). The cyclopropanation of olefins in the presence of irradiated CH_2I_2 however was reported in diluted solvent−olefin mixtures[18−20] indicating that the reaction is much slower as compared with the tens of picosecond time domain of vibrational cooling of neutral polyatomic molecules in solution.[36,37]

The present work is concerned with the femtosecond and nanosecond photolysis of CH_2I_2 at 266 and 310 nm in various solvents (*n*-hexane, dichloromethane, acetonitrile, methanol, and ethanol). We mainly focus on (1) the quantitative evaluation of the quantum yield of the isomer formation upon 266-nm excitation; (2) the investigation of decomposition and thermal stability of CH_2I-I in solution because this isomer is apparently not stable enough to be detected via steady-state spectroscopy; (3) the investigation of CH_2I-I reactivity toward cyclohexene. Our main results are as follows. The time scale and quantum yield of CH_2I-I formation are largely solvent independent. On the contrary, the thermal stability of CH_2I-I depends strongly on the solvent. We show through direct observations that the species reacting with olefins (cyclohexene) in irradiated solutions of CH_2I_2 is the vibrationally cold CH_2I-I isomer.

2. Experimental Section

2.1. Materials. CH_2I_2 (> 98%, Fluka), solvents (Merck, p.a.), and cyclohexene (Aldrich, 99+%) were used as received. All experiments were performed at 21 ± 1 °C unless stated otherwise. All UV−visible spectra were recorded using JASCO V-530 spectrophotometer.

2.2. Femtosecond Spectrometer. This setup is based on a 1 kHz Ti:sapphire laser/regenerative amplifier system producing ∼100 fs, 0.9 mJ pulses at 800 nm.[38−40] The amplified beam is split 65:35%. The 65% part is used to pump a frequency tripler for creating the 266-nm excitation pulses or an optical parametric amplifier (OPA) to produce the 310-nm pulses used for excitation in solvents other than acetonitrile. The variably time-delayed excitation pulses were ∼5 μJ (266 nm) and ∼2 μJ (310 nm) in energy at the sample. The 35% part is used directly or after attenuation to produce the probe, either as single-wavelength light from a second OPA between 280 and 380 nm or as a white-light continuum in the 330−860 nm region.[40] The probe is split into the identical probe and reference beams, which are passed through the sample, dispersed by a monochromator/spectrograph, and then detected in a two-photodiode or dual photodiode array arrangement in combination with a gated pump photodiode. The excitation beam is chopped at 500 Hz. The excitation-induced change in a decadic absorbance of the sample (ΔA) is calculated from the probe-to-reference signal ratios for

alternate laser shots, as described earlier,[41] and averaged over 500 pairs of the laser shots for each delay time and several scans. Pump and probe beams cross in the sample at angle of ~8°. The relative polarization of the pump and probe pulses is set to the magic angle (54.7°). For measurements of transient spectra and yields, the sample was a solution containing CH_2I_2 (55 or 15 mM, respectively) flowed through a 0.2 mm path length Spectrosil quartz cell. Transient spectra were acquired in overlapping spectral regions (typically ~270 nm), corrected for dispersion of the probe light and combined together after scaling. Two-photon absorption signals in flowing neat methanol[39] yielded time zero at different probe wavelengths and an instrument response function of 200 fs (fwhm of a Gaussian fit). Samples of CH_2I_2 (0.4, 1, and 2 mM) in acetonitrile were flowed through a 1 mm cell.

2.3. Nanosecond Laser Photolysis. The spectrometer has been described previously.[42] The 266-nm photolysis light was the quadrupled output of a Nd:YAG laser. It could be varied in the 0.01−1.1 mJ pulse^{-1} range using a polarizer. The probe light from a pulsed Xenon arc lamp was passed through the sample and two monochromators and was subsequently detected with a photomultiplier tube. A Xe-lamp flash had no influence on the transients produced by photolysis. The apparatus response function (~11 ns fwhm) allowed for a time resolution of ~3 ns after deconvolution. The 310-nm light used to excite cyclohexene−solvent mixtures was obtained by frequency-doubling the 620-nm output from an OPO pumped by the 355-nm output from the Nd:YAG laser. The CH_2I_2 (3.1−9.3 mM) samples were flowed through a 1 mm Spectrosil quartz cell and deoxygenated by bubbling with O_2-free argon. Low concentrated CH_2I_2 samples (0.25−1 mM) were contained in a sealed O_2-free 1 cm cuvette equipped with a magnetic stirring bar. The temperature dependencies of the reaction rates were studied from 5 to 55 °C in the sealed 1 cm cuvette placed in a thermostated holder.

2.4. Quantum Yield. The formation quantum yields of the CH_2I-I product (Φ_i) following 266-nm photolysis were determined with the help of eq 2

$$\Phi_i = \frac{\Delta A}{\epsilon} N_A 10^{-3} \frac{Fh\nu(\pi r^2)}{E(1-10^{-A})} \qquad (2)$$

where ΔA and ϵ are the absorbance and extinction coefficient of CH_2I-I at the probing wavelength, E and $F = 1.04$ are the incident excitation energy and its measured loss due to reflection off the cell front window, A is the sample absorbance at 266 nm, $h\nu = 7.466 \times 10^{-19}$ J is the 266-nm photon energy, $N_A = 6.022 \times 10^{23}$ mol^{-1} is the Avogadro number, and r is half of the "equivalent diameter" [43] of the excitation beam at the sample position. The Gaussian 2D beam profiles were measured using a linear CCD array or a movable pinhole. The $r = 9.5 \times 10^{-3}$ cm (femtosecond) and $r = 9.5 \times 10^{-2}$ cm (nanosecond) values were calculated from transmission measurements of the beams through pinholes for a set of varying diameters using the equation of Dietz and Merlin.[43] The corresponding probe beams were smaller by a factor of ~2. In all of the experiments, the number of excitation photons absorbed by the sample was within the error bars when deduced either from the pulse energies measured before and after the sample or from the Lambert−Beer law.

3. Results and Discussion

3.1. Steady-State Spectrum. Absorption of CH_2I_2 in CH_3CN and n-C_6H_{14} is shown in Figure 1. The spectra in other investigated solvents[44] and the gas-phase spectrum[45] fall between, suggesting the same orbital nature of the electronic transitions. CH_2I_2 obeys the Lambert−Beer law in the concentration range ~0.2−100 mM (Figure 1, insets).

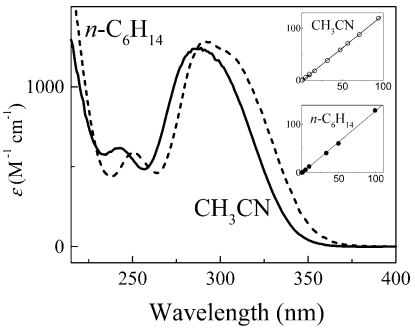

Figure 1. UV absorption spectra of CH_2I_2 in acetonitrile and n-hexane. Insets: the plots of the measured absorbance at $\lambda = 290$ nm corrected for the cuvette path length versus CH_2I_2 concentration (in mM).

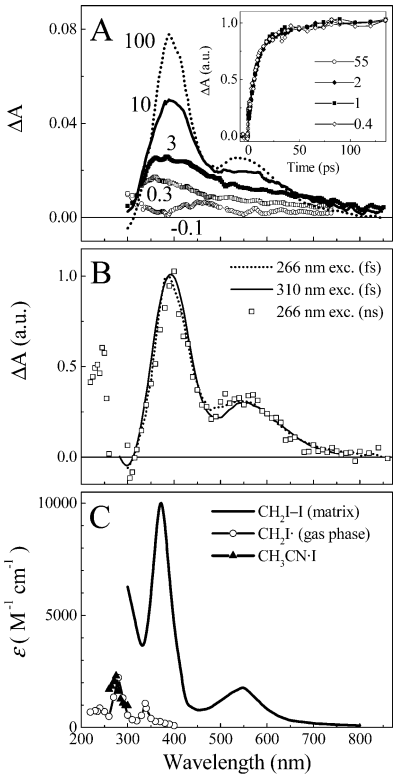

Figure 2. (A) Transient absorption spectra of CH_2I_2 in CH_3CN after 266-nm excitation. Time delays between the pump and the probe pulses (in picoseconds) are given beside each spectral curve. Inset: the superimposed 400-nm kinetic traces for samples containing 0.4, 1, 2, and 55 mM of CH_2I_2. The measured points at ±250 fs around zero time for the 0.4−2 mM samples were identified as partly due to the solvent and removed. (B) Normalized at the UV peak transient spectra of CH_2I_2 in CH_3CN, which were measured 200 ps after 310-nm (solid line)[2] or 266-nm excitation (dot line), and at 0 ns delay with respect to the 266-nm pulse following nanosecond photolysis (squares). The 266-nm spectra are from this work. (C) The literature data on absorption of CH_2I-I in N_2 matrix at 12 K,[27] gas-phase $CH_2I^{\bullet}$,[46] and a charge-transfer complex with the solvent, $CH_3CN{\cdot}I$.[49]

3.2. Identification of an Early Photolysis Intermediate, the CH_2I-I Isomer. Figure 2a displays the absorption changes for CH_2I_2 in acetonitrile caused by a 266-nm photon from −0.1 to 100 ps. The spectral evolution resembles that upon 310-nm femtosecond (fs) photolysis of CH_2I_2,[2] and therefore is interpreted similarly. The pulse-limited rise of transient absorption followed by ~120−150 fs decay is due to the population of

the Franck−Condon region of the CH_2I_2 excited state by the pump pulse and its depopulation as a result of dissociation.[8,11] The broad absorption between 0.2 and 3 ps is composed of two subbands at ∼430 nm (shifts to ∼400 nm with time) and ∼350 nm, which are assigned to the CH_2I-I product (being present already at ∼1 ps), and the $CH_2I^•$ photofragment, respectively. Two 394 and 558 nm product bands arise through growth and spectral narrowing from 3 to 100 ps and remain unchanged to the longest measured delay 500 ps. These bands are similar to the bands obtained after 200 ps following 310-nm excitation (Figure 2b) and all belong to the vibrationally relaxed ground-state CH_2I-I isomer (Figure 2c). Like we observed for the same sample but at the 320-nm pump and 420-nm probe wavelengths,[2] the temporal profile of the 400-nm transient (Figure 2a, inset) is independent of CH_2I_2 concentration in the 0.4−55 mM range, in disagreement with the Saitow et al. studies.[16] The development of the 394 and 558 nm bands, as we would like to emphasize here, is associated with a slow increase of CH_2I-I concentration mixed with vibrational relaxation. By applying the conservation rule of the electronic transition dipole strength,[47] a ∼5.5 ps rise time of the CH_2I-I concentration is found from the frequency-integrated intensities of the ∼390 and ∼560 nm bands. A rise of absorption at these central wavelengths and a more rapid reduction of absorption at the wings of the bands (the narrowing), the typical dynamics observed for vibrationally relaxing small molecules,[36,48] suggests that CH_2I-I is formed internally hot. The narrowing takes place on two distinct time scales of several picoseconds and several tens of picoseconds and is largely complete at ∼75−100 ps, indicating the formation of the equilibrated CH_2I-I isomer. No transient absorption evolution was observed that could be associated with reformation of the parent CH_2I_2 molecule in acetonitrile. For CH_2I_2 in other solvents, 310-nm excitation was carried out to minimize two pump photon absorption by the solvent.[39] The formation of CH_2I-I and similar dynamics within the isomer bands (somewhat faster in polar solvents) were observed. At 100 ps, the transient absorbance measured at 390 nm was comparable in all investigated solvents, whereas a change in intensity (and somewhat in position) of the visible band with solvent polarity was observed under identical experimental conditions.

Following nanosecond photolysis of CH_2I_2 (9.3 mM) at 266 nm, absorption spectra with two maxima at ∼390 nm and ∼560−570 nm develop with a pulse-limited rise time in all of the solvents investigated, see Figures 3−5 for *n*-hexane, acetonitrile, and methanol. The characteristics of the spectra are presented in Table 1. These spectra are assigned to the CH_2I-I photoproduct as they are indistinguishable from the 100−200 ps spectra of the equilibrated isomer (Figure 2b compares these spectra for the solvent CH_3CN). The nanosecond CH_2I-I isomer is not formed through diffusion of a $CH_2I^•$ radical and an $I^•$ atom[56] and likely is the same as that observed in the ultrafast experiments. The intensity of the ∼390 nm band was essentially the same in *n*-C_6H_{14}, CH_2Cl_2, and CH_3CN under identical conditions. Charge-transfer (CT) complexes of $I^•$ with solvent molecules (solvent·I) are known to be formed on the subpicosecond time scale.[57] Their absorption for the solvents investigated here is approximately bell-shaped peaking at $\lambda \leq 360$ nm (Figures 2, 3, and 5).[49,50,55] Iodomethyl radicals contribute to the transient absorption in deoxygenated solutions at $\lambda \leq 360$ nm, as confirmed by experiments in the presence of oxygen ($CH_2I^•$ is quenched rapidly by O_2, $k \sim 10^9$ M^{-1} s^{-1} [58]). A weak absorption in this region immediately after photolysis suggests that $CH_2I^•$ and $I^•$ radicals are produced in small yields relative to that of CH_2I-I.

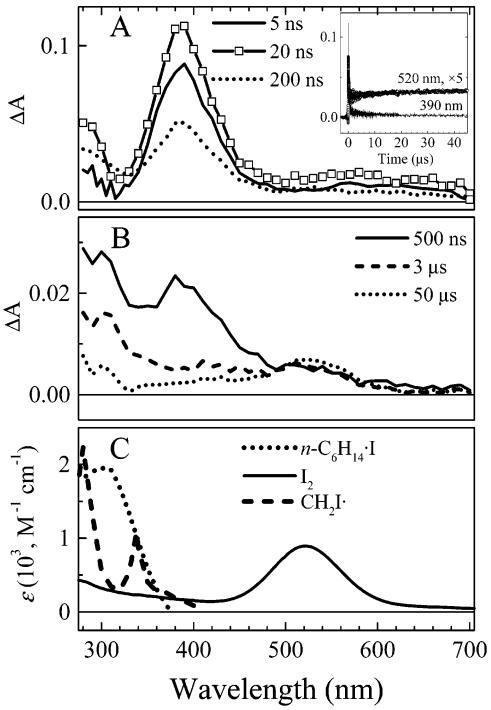

Figure 3. (A and B) Transient absorption spectra obtained following 266-nm nanosecond photolysis (0.5 mJ $pulse^{-1}$) of CH_2I_2 in deoxygenated *n*-hexane. Inset: the kinetics at 390 and 520 nm. (C) Absorption of *n*-C_6H_{14}·I,[50] gas-phase $CH_2I^•$,[46] and I_2 in *n*-hexane.

TABLE 1: Spectroscopic Properties, Quantum Yields for Formation, and Observed Decay Rates of the CH_2I-I Isomer Produced Following 266-nm Nanosecond Photolysis of CH_2I_2

	spectral data					
solvent	λ_{UV} (nm)	λ_{vis} (nm)	I_{UV}/I_{vis}[a]	k_{obs}^{-1} (ns)[b]	ϵ_s (M^{-1} cm^{-1})[d]	Φ_i (%)[e]
CH_3CN	394	558	3.3	45[c]	5590 ± 500	69 ± 11[f]
n-C_6H_{14}	386	572	6.1	180	6860 ± 620	75 ± 11
CH_2Cl_2	391	562	3.95	220	6090 ± 250	94[g]
CH_3OH	391	558	3.75	5[c]	6140 ± 610	74 ± 8
C_2H_5OH	391	560	4.2	8[c]	7140 ± 890	89[g]

[a] The intensity ratio of the UV and visible absorption bands in the transient spectra acquired within or immediately after the photolysis pulse. [b] The observed decay rate of CH_2I-I under similar photolysis conditions ($[CH_2I_2] = 9.3$ mM, energy 0.4−0.6 mJ $pulse^{-1}$). The kinetic traces were measured at the UV and visible band maxima, fitted to two or three exponentials and the fastest decay rate was taken as k_{obs}. [c] From deconvolution of the 390-nm kinetic traces with the apparatus response function. [d] Maximum extinction coefficient of the isomer UV band. The standard error of the mean is determined by the error bars of Gaussian fits of the spectra, section 3.4. [e] Based on eq 2 for CH_2I_2 (9.3 mM). Error bars represent experimental error and do not contain the inaccuracy of ϵ_s. In CH_3CN and *n*-C_6H_{14}, the same Φ_i were obtained within the error bars for CH_2I_2 3.1 and 9.3 mM. [f] The use of the benzophenone triplet state as a transient actinometer in nanosecond photolysis yields $\Phi_i = 73 \pm 7\%$. From femtosecond photolysis of CH_2I_2, eq 2 yields $\Phi_i = 69 \pm 15\%$. [g] Single determination; estimated error ± 15%.

The origin of two-band product absorption spectra for CH_2I_2 (see the Supporting Information) has been discussed elsewhere,[2,59] so only $CH_2I^•$ [15] and $CH_2I_2^+$ [16,34] assignments made for photoexcitation of liquid-phase CH_2I_2 are discussed below in light of the new results. The $CH_2I^•$ nature of the ∼560 nm band[15] is inconsistent with its decay parallel to that of the ∼390 nm band, insensitivity toward O_2 (section 3.6), and ab initio calculations.[32,60] As to $CH_2I_2^+$, direct one-photon production of $CH_2I_2^+$ with $h\nu \sim 4.66$ eV is not possible for nonaggregated

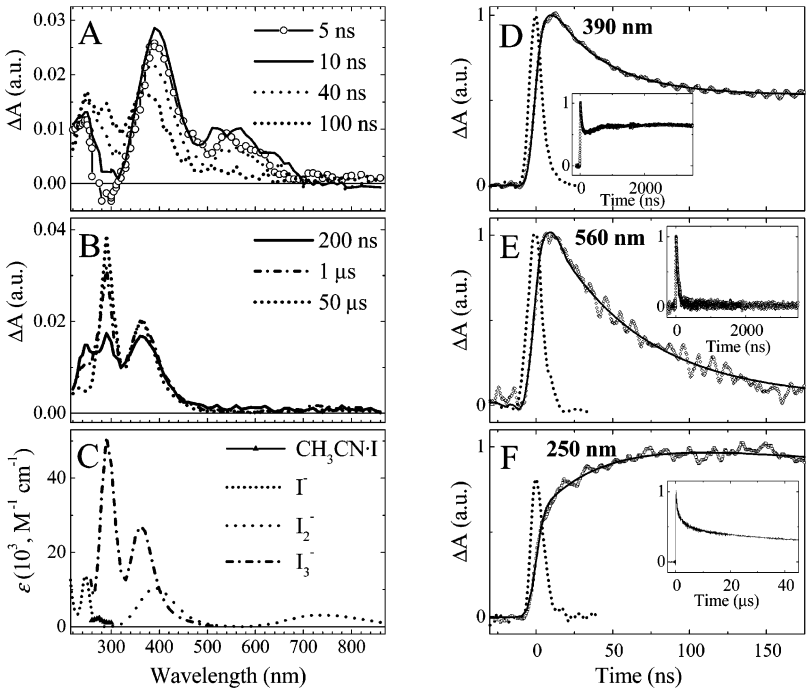

Figure 4. 266-nm nanosecond photolysis (0.6 mJ pulse^{-1}) of CH_2I_2 in deoxygenated CH_3CN. (A and B) Measured transient absorption spectra. (C) Absorption of I_2^- in methanol[51] (note, absorption of I_2^- and I_3^- is little affected by the solvent[52]), $CH_3CN{\cdot}I$,[49] I^-,[53] and I_3^-[54] in acetonitrile. (D, E, and F) Kinetics (symbols) recorded at 390, 560, and 250 nm. The solid lines are two-exponential fits convoluted with the apparatus response function (dots). Insets: the same kinetics over 4 μs (390 and 560 nm) and 50 μs (250 nm) time spans.

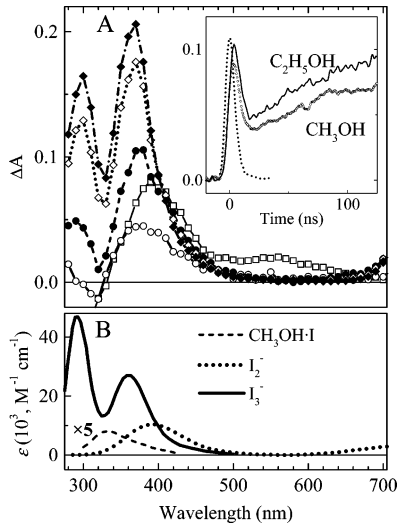

Figure 5. (A) Transient spectra measured 0 ns (□), 20 ns (○), 200 ns (●), 3 μs (◇), and 50 μs (◆) after 266-nm nanosecond photolysis (0.6 mJ pulse^{-1}) of CH_2I_2 in deoxygenated methanol. Inset: the 390-nm kinetics obtained for CH_2I_2 in methanol and ethanol during the first 100 ns. (B) Absorption of $CH_3OH{\cdot}I$,[55] I_2^- in methanol,[51] and I_3^- in ethanol.[54]

CH_2I_2 (ionization potential of CH_2I_2 is 9.46 eV[61]). If CH_2I_2 molecules were to aggregate, the possibility for the $CH_2I_2^+$ formation could exist.[16] Our transient (Figure 2a, inset) and steady-state (Figure 1, inset) absorption data do not support aggregation of CH_2I_2. $CH_2I_2^+$ was also suggested to be formed via two-(266 nm) photon absorption in a cyclohexane solution of CH_2I_2 and to contribute significantly to the ~560 nm band.[34] However, we note that absorption of $CH_2I_2^+$ at 560 nm disagrees with ab initio,[32] photoelectron, and collision spectroscopy results.[62,63] The contribution of $CH_2I_2^+$ to the ~560 nm product band for our experiments can be ruled out because of the following reasons: (1) The excitation level is too low to cause two-photon or stepwise excitation of CH_2I_2 (excitation energy flux (2−3) × 10^{16} photons cm^{-2} pulse^{-1}) and its attenuation by a factor of 50 resulted in a linear reduction of transient absorbance within the bands in nanosecond (*n*-C_6H_{14}) and femtosecond (CH_3CN) photolysis. (2) The instantaneous intensity of the laser pulses differs by 5 orders of magnitude in these techniques, yet the amplitude ratio of the ~390 and ~560 nm bands is the same (Figure 2b). Therefore, the CH_2I-I isomer produced in a one-photon process is responsible for both the ~390 and ~560 nm bands observed in the present study and not the $CH_2I^{\bullet}$ radical or the $CH_2I_2^+$ cation.

3.3. Nature of Two-Band Absorption of CH_2I-I. The absence of quenching by O_2, the large ϵ ~6500 M^{-1} cm^{-1} (sections 3.6 and 3.4), and modest solvatochromism of the ~390 nm band of CH_2I-I probably indicates a singlet-to-singlet transition associated with no appreciable intramolecular charge-transfer. The spectra in various solvents of this work strongly support the original assignment[26] of the long-wavelength (~560−570 nm) band of CH_2I-I to a CT transition from the "iodide ion" to the "carbenium ion". Among resonance structures suggested for the CH_2I-I species, the contact ion pairs ($H_2C^+-I^{\cdots}I^-$ and $H_2C{=}I^{+\cdots}I^-$) have been concluded to be more important than the less polar halonium ylide, the carbene−molecular halogen complex, the hypervalent species, the contact ion pair with decoupled double bond, and the radical pair.[27] An increase of solvent polarity should stabilize $H_2C^+-I^{\cdots}I^-$ and $H_2C{=}I^{+\cdots}I^-$. This would increase the relative strength of the long-wavelength CT transition upon going from *n*-C_6H_{14} to CH_2Cl_2 and CH_3CN, as we observed. The accompanying blue shift is not large (~440 cm^{-1}) probably because the CT interaction in CH_2I-I is quite strong so the difference in dipole moments between ground and excited states is not large, so the solvent stabilization energy difference between ground and excited states is small (Chapter 6 of ref 64).

3.4. Quantum Yield of CH_2I-I Formation upon 266-nm Excitation. The extinction coefficient of equilibrated CH_2I-I in solution is estimated from the known spectrum of CH_2I-I

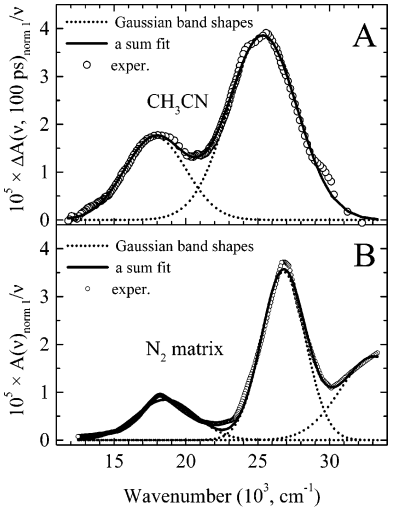

Figure 6. Absorption of CH_2I-I and the corresponding fits to Gaussian band shapes. The isomer spectra recorded: (A) 100 ps following 266-nm photolysis of CH_2I_2 in acetonitrile at 294 K; (B) after irradiation of CH_2I_2 in N_2 matrix at 12 K.[27]

in cold N_2 matrices[26,27] on the basis of the conservation rule of the transition dipole strength (Chapter 3, ref 64) for the UV absorption band, which can be written as

$$n_M\epsilon_M\int_{band}G_M(\nu)\,d\nu = n_S\epsilon_S\int_{band}G_S(\nu)\,d\nu \qquad (3)$$

Here, υ is the wavenumber in cm^{-1}, $n_{S,M}$ are the refractive indices of the solvent[65] and N_2 matrix ($n_M = 1.30$[66]), and $\epsilon_{S,M}$ and $G_{S,M}(\upsilon)$ are the maximum extinction coefficients and the band shapes of the UV band for the solution and matrix ($\epsilon_M \approx 10\,000\ M^{-1}\ cm^{-1}$ [26,27]). The $G_{S,M}(\upsilon)$ band shapes are obtained by least-squares fitting the isomer absorbance (in the form $\Delta A(\nu,t)_{norm\,1}\ \nu^{-1}$) to a sum of two Gaussians (a third band shape is added at $\nu > 30\,000\ cm^{-1}$ to fit the matrix spectrum) of variable area, central frequency and width. This approximation is reasonable based on transition energy calculations for CH_2I-I,[32,60] and the fits are satisfactory (Figure 6). For CH_2I-I in CH_3CN, eq 3 gives $\epsilon_S = 5590 \pm 500\ M^{-1}\ cm^{-1}$. In the other solvents, the spectra recorded between −5 and 10 ns with respect to the nanosecond photolysis pulse were Gaussian-fitted. Analysis of these spectra showed that the UV band is symmetrically bell-shaped and not skewed in the direction of shorter λ. This would be the case if the radical contribution were significant (cf. the 0 and 20 ns spectra, Figure 5). The ϵ_s obtained are in the 6170−7100 $M^{-1}\ cm^{-1}$ range and summarized in Table 1.

Following the femtosecond 266-nm excitation of CH_2I_2 in acetonitrile, the formation quantum yield of CH_2I-I ($\Phi_i = 69\%$) was determined via eq 2 from the slope $\Delta A(380\ nm)/E = 1.27 \times 10^4\ J^{-1}$ at 100 ps delay. The observed dynamics suggest that CH_2I-I is formed through in-cage recombination not later than $3\tau \approx 18$ ps after excitation of CH_2I_2, where $\tau = 5.5$ ps and is the slower formation time constant of CH_2I-I. Unity quantum yield for the C−I bond breaking in CH_2I_2 has been suggested.[3,4] Hence the Φ_i determined is equivalent to recombination into the isomer of ∼70% of the $CH_2I^\bullet$ and $I^\bullet$ photofragments. Following the nanosecond 266-nm photolysis, the Φ_i values were calculated to be between 69 and 94% depending on solvent (Table 1) with the use of 390-nm kinetic traces deconvoluted with the apparatus response function. The photochemical isomer yield is found to be independent upon variation of the incident excitation energy in the range ∼0.015−0.9 and ∼0.2−1.1 mJ pulse^{-1} in *n*-C_6H_{14} in CH_3CN, respectively, suggesting that secondary photolysis of initial transients is negligible. The yield obtained in CH_3CN was further confirmed using the triplet state of benzophenone as an actinometer (Table 1, footnote f). The benzophenone triplet is known to have $\epsilon(525\ nm) = 7800\ M^{-1}\ cm^{-1}$ and be formed with unity quantum yield upon excitation at 266 nm.[67] The Φ_i values obtained from femtosecond and nanosecond photolysis of CH_2I_2 in CH_3CN agree within the error limits suggesting that secondary geminate recombination of $CH_2I^\bullet$ and $I^\bullet$ into CH_2I-I is not important. This agrees with the absence of a tens-of-picoseconds rise in the integrated absorption of CH_2I-I that would correspond to such recombination.

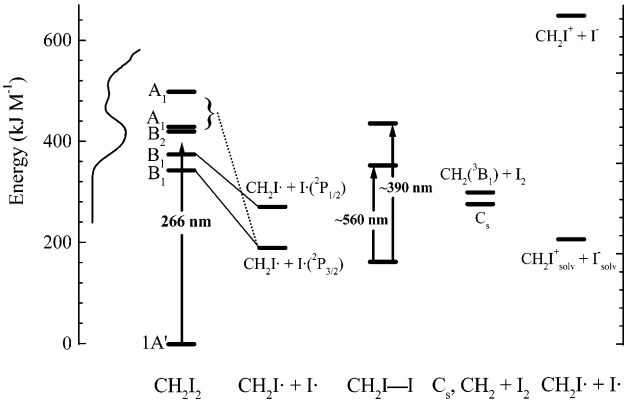

Figure 7. Energetics of the CH_2I_2 system. The energies are expressed with respect to ground-state CH_2I_2. The absorption spectrum of CH_2I_2 is shown adjacent to the energy axis. The assignments and correlations of the excited states of CH_2I_2 are from El-Sayed and co-workers.[7] The energy of the $CH_2I^\bullet + I^\bullet(^2P_{3/2})$ radical pair is from experiment.[68] The G2:MP2/6-31G(d) energies are used for ground-state CH_2I-I, the $CH_2I_2 \rightarrow CH_2(^3B_1) + I_2$ dissociation and the transition state (Cs) for the $CH_2I_2 \rightarrow CH_2I-I$ isomerization.[28] The energy of CH_2I^+ and I ions is 722 kJ mol^{-1} in gas phase and 232 kJ mol^{-1} when infinitely separated and solvated in the solvent CH_3CH (see this section).

3.5. Thermodynamics of Bond-Breaking in CH_2I_2. The energy diagram of CH_2I_2 is presented in Figure 7, and the relevant energies are collected in Table 2. The enthalpy change for $CH_2I_2 \rightarrow CH_2I^\bullet + I^\bullet(^2P_{3/2})$ has been obtained experimentally.[68] It is added with the spin−orbit splitting of the iodine atom (7590 cm^{-1}) to obtain the relative energy of the $CH_2I^\bullet + I^\bullet(^2P_{1/2})$ dissociation channel. The enthalpy change for the $CH_2I_2 \rightarrow CH_2I-I$ isomerization is that computed using the G2 scheme with the MP2/6-31G(d) geometries.[28] This is preferred over the enthalpy change based on the DFT (B3LYP/Sadlej-PVTZ) approach,[30] because some density functionals (e.g., B3LYP) have been reported to grossly underestimate the thermodynamic stability of closed shell haloalkanes.[69] Using G2, an enthalpy change of about 20 kJ mol^{-1} separates ground-state CH_2I-I and the radical pair $CH_2I^\bullet + I^\bullet(^2P_{3/2})$ state, and other decomposition routes of the isomer to $CH_2(^3B_1) + I_2$ and CH_2I_2 are noticeably higher in energy,[28] Figure 7. The enthalpy change for gas-phase heterolysis of ground-state CH_2I_2 to form $CH_2I^+ + I^-$, $\Delta H_{het}(CH_2I_2)$, is 722 kJ mol^{-1} (Table 2, footnote h). On the basis of thermodynamics data, homolysis of the C−I bond followed by electron transfer in the resulting radical pair and heterolysis to produce $CH_2I^+ + I^-$ without solvation are strongly uphill for CH_2I_2 excited with 266 nm light ($h\upsilon = 449$ kJ mol^{-1}).

Solvation of the product ions in the solvents CH_3CN, CH_3OH, and C_2H_5OH is a possibility to reduce the energy demand for dissociation of CH_2I_2 into $CH_2I^+ + I^-$. To evaluate the effect of solvation on the energetics of the CH_2I_2 system, we estimated the total solvation energy (ΔG_s) of the completely separated and solvated CH_2I^+ and I^- ions and assumed, as usual, that

TABLE 2: Thermodynamic Parameters for the C−I Bond Dissociation in CH_2I_2 in Acetonitrile and Alcohols[a]

solvent	ΔG_s° (I^-)[b]	ΔG_s° (CH_2I^+)[c]	ΔH $(CH_2I^\bullet + I^\bullet)$[d]	ΔH_{het} (CH_2I_2)[h]	ΔG[i]	ΔH (CH_2I-I)[j]	I^- (%)[n]
gas phase			212.9[e] 194.8[f] (197.0)[m] 178.6[g] (180.8)[m]	722		175.4[k] (182.0)[m] 169.0[l] (175.6)[m]	
CH_3CN	−266.5	−224.3			232		20
CH_3OH	−275.9	−228.6			218		23
C_2H_5OH	−270.3	−216.5			236		16

[a] The free energies and bond dissociation enthalpies are in kJ mol^{-1}. Unless stated otherwise, all energy-related values pertain to 298 K. [b] Calculated with use of the free energy of hydration (g−H_2O) and of transfer (H_2O−solv).[70] [c] MSA calculation. [d] The C−I bond dissociation enthalpies of CH_2I_2. [e] Mass-spectroscopy experiment.[68] [f] G2, 0 K.[28] [g] CASSCF, 0 K,[30] for $CH_2I_2 \rightarrow CH_2I^\bullet + I^\bullet(^3P)$. [h] By use of appearance potential of CH_2I^+ (10.55 eV[71]) following the $CH_2I_2 \xrightarrow{h\nu} CH_2I^+ + I + e^-$ fragmentation and electron affinity energy of iodine (3.06 eV[61]). [i] Calculated as $\Delta H_{het}(CH_2I_2) + \Delta G_s^\circ(I^-) + \Delta G_s^\circ(CH_2I^+)$. [j] The enthalpy change for the $CH_2I_2 \rightarrow CH_2I-I$ isomerization. [k] G2, 0 K.[28] [l] B3LYP, 0 K.[30] [m] Temperature-corrected to 298 K using standard formulas of statistical mechanics and harmonic frequencies[32] with one extra translational degree of freedom for the radical route. [n] I^- yield is counted (low limit) assuming that I^- produces an equal amount of I_3^- and I_2^- ions at long-time after photolysis (50 μs), 294 K.

homolysis in solution is well described by the gas phase thermodynamic data. The liquid phase heat of heterolysis (ΔG) of CH_2I_2 into $CH_2I^+ + I^-$ equals $\Delta H_{het}(CH_2I_2) + \Delta G_s$, where $\Delta H_{het}(CH_2I_2) = 722$ kJ mol^{-1} and $\Delta G_s = \Delta G_s^\circ(I^-) + \Delta G_s^\circ(CH_2I^+)$, with the latter two being the standard molar solvation energies of the I^- and CH_2I^+ ions. The $\Delta G_s^\circ(I^-)$ and $\Delta G_s^\circ(CH_2I^+)$ energies are collected in Table 2. $\Delta G_s^\circ(I^-)$ are calculated using the free energies of hydration (gas−H_2O) and of transfer (H_2O−solvents), available in the literature.[70] $\Delta G_s^\circ(CH_2I^+)$ is dominated by a long-range electrostatic contribution to the solvation energy of the ion. This was obtained in the mean spherical approximation (MSA)[72] using the hard sphere radii of CH_2I^+ ($r_s = 2.25$ Å[73]) and of the solvent (r_v) and by use of the solvent static dielectric constant (D).[77] The obtained ΔG_s and ΔG were comparable in all three solvents (Table 2). As a result, the infinitely separated and solvated CH_2I^+ and I^- ions lie ∼20 kJ mol^{-1} above the $CH_2I^\bullet + I^\bullet(^2P_{3/2})$ threshold and ∼40 kJ mol^{-1} above ground-state CH_2I-I (Figure 7). Generally, forces other than electrostatic ion dipole forces may play an important role in solvation, e.g., short-range electron-pair donor acceptor forces,[65,70] which are not considered here. They may increase the solvation energy of CH_2I^+ in the pronounced electron-pair donors CH_3OH and C_5H_5OH and, to a lesser extent, in the weak donor CH_3CN.

To understand why CH_2I_2 excited with a low-energy UV photon undergoes homolysis even in solvents capable of providing a significant solvation energy of an ion, the picture assumed in the literature,[14,17] the following should be noted. Because the absorption spectrum of CH_2I_2 in polar solvents is comparable to that in the gas phase, the presence of optical electron transfer absorption can be ruled out. The degree of heterolysis as compared to homolysis on a time scale of bond breaking depends on whether the energy of the transition state for the incipient ions is lowered significantly by solvation. In CH_3CN, about 70% of the solvation energy change occurs with a time constant of 90 fs and another 30% is slower (630 fs).[78] In CH_3OH and C_2H_5OH, fast solvation (30 fs) is responsible for only about 10% of the total solvation energy change, whereas other solvation components are significantly slower.[78] C−I heterolysis of CH_2I_2 upon excitation with a 266-nm photon is 270 kJ mol^{-1} endothermic (without solvation), and a very significant portion of subpicosecond and picosecond solvation has to occur before the heterolysis can take place. As the $CH_2I^\bullet$ photofragment is spectroscopically detected already at ∼200 fs, we conclude that CH_2I_2 excited at $\lambda_{exc} = 266$ nm should undergo homolysis in the alcohols and predominantly in acetonitrile. In the formed $CH_2I^\bullet + I^\bullet$ radical pair, electron transfer (concerted with solvation of the incipient ions) seems to be plausible on energy ground, but because recombination of $CH_2I^\bullet$ and $I^\bullet$ into CH_2I-I would be in dynamic competition with the electron transfer, the relative invariance of the isomer quantum yield in solvents of drastically different polarity suggests that this process is improbable.

3.6. Decay of CH_2I-I. Both short- and long-wavelength absorption bands decay with the same rate as expected. The initial phase of the decay is unaffected and the long times are only slightly affected by the presence of O_2. The isomer decay is followed by formation of secondary products that are noncharged species in CH_2Cl_2 and n-C_6H_{14} and also involve ions in the more polar CH_3CN, CH_3OH, and C_5H_5OH. As investigated in CH_3CN, CH_2Cl_2, and n-C_6H_{14}, the decay rate of CH_2I-I increases upon increase of its initial concentration (denoted as $[CH_2I-I]$), which was varied by a change in photolysis energy and/or CH_2I_2 concentration. This suggests the presence of second-order reactions between CH_2I-I and photolysis products. At similar CH_2I_2 concentration and excitation energy (spectra in Figures 3−5), the observed decay rates of CH_2I-I (k_{obs}) can be compared and their solvent dependencies are summarized in Table 1.

3.6.1. n-Hexane and Dichloromethane. Figure 8a presents the plot of k_{obs} versus $[CH_2I-I]$ in n-hexane at 21 °C. The rate data were fitted to the power law equation, $k + k_1 \times [CH_2I-I]^{1/2}$, where k is the first-order (intramolecular) decay rate. The resultant fitting parameters are $k_1 = (3.7 \pm 0.8) \times 10^6$ $M^{-1/2}$ s^{-1} and $k = (1.8 \pm 0.4) \times 10^5$ s^{-1} (5.5 μs lifetime). Measurements in CH_2Cl_2 yielded similar rates (Figure 8a). Activation energy of the isomer decay process was evaluated as follows. The isomer decay rates for samples of CH_2I_2 (1 mM) in n-hexane were measured between 5 and 55 °C in a low initial concentration region (corresponding to a relatively flat part of the k_{obs} vs $[CH_2I-I]$ plot in Figure 8a). The Arrhenius plots of k_{obs} at three different photolysis energies (hence, starting isomer concentrations) showed the same apparent activation energy of 41 ± 2 kJ mol^{-1}. When extrapolating k_{obs} to $[CH_2I-I] = 0$, the activation energy of 42 ± 8 kJ mol^{-1} is obtained.

As CH_2I-I decays in CH_2Cl_2, the isobestic point is observed at 349 nm out to 100 ns after photolysis (not shown), suggesting one pathway mechanism for the isomer decomposition. The production of $CH_2I^\bullet$ radicals in this step in the solvents CH_2Cl_2 and n-C_6H_{14} is confirmed by experiments in the presence of oxygen. Under the assumption that one decayed CH_2I-I produces one $CH_2I^\bullet$, the ϵ of $CH_2I^\bullet$ is the same as that of CH_2I-I (∼1400 M^{-1} cm^{-1}) at $\lambda = 349$ nm, i.e., comparable with the ϵ in the gas-phase radical 338-nm band (1075 M^{-1} cm^{-1} [46]). This and a rapid decrease of ϵ of $CH_2I^\bullet$ to 370 nm determined from the 0−100 ns spectra suggest that the 338-nm band undergoes a red shift to ∼350 nm (∼1100 cm^{-1}) in solution, in agreement with the ∼345 nm absorption of $CH_2I^\bullet$ in acidic water.[79] The

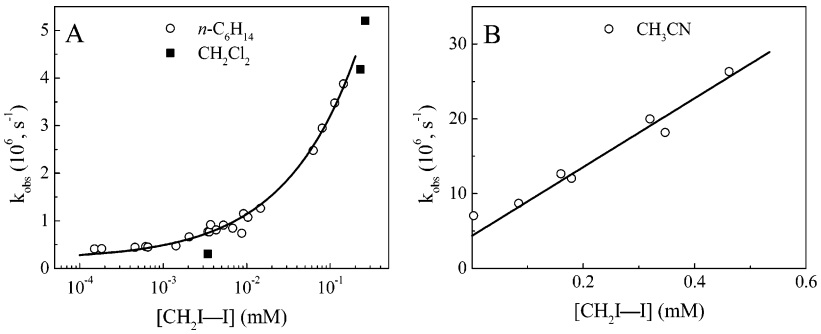

Figure 8. Observed decay rate of CH_2I-I (symbols) plotted against its initial concentration, which is determined from ϵ and absorbance of the isomer at $\lambda = 390$ nm immediately after the 266-nm photolysis pulse. (A) For the solvents *n*-hexane and dichloromethane. The line is the fit of the *n*-hexane data (note $[CH_2I-I]$ is plotted on a log axis). (B) For the solvent acetonitrile. The line is the linear fit to the rate points.

ΔA decreases at $\lambda < \sim 315$ nm as CH_2I-I decays indicating the presence of the isomer absorption in this region (Figure 3). The ϵ of CH_2I-I at 285 nm ($\sim$2000 M^{-1} cm^{-1}) and 300 nm ($\sim$1000 M^{-1} cm^{-1}) were estimated from fitting the 5-ns spectrum to two Gaussians, the spectra of *n*-C_6H_{14}•I, CH_2I_2 and gas-phase CH_2I• (the estimated ϵ were only weakly sensitive to CH_2I• absorption). CH_2I-I is a precursor of a broad composite absorption extending from 310 to 450 nm (Figure 3), which decays gradually while I_2 develops for $t > \sim 500$ ns. Only produced I_2 and depleted CH_2I_2 absorption were observed after 10 ms. The composite absorption is due to *n*-C_6H_{14}•I and, in both solvents, CH_2I• and a new product species ($\tau_{1/2} \approx 4$ μs) with a band between 370 and 450 nm peaking at 400−410 nm and a less distinguishable band at $\sim$330−340 nm. We tentatively assign this species to CH_2I_2•I, in accord with the $\sim$390 nm absorption attributed to RI•I[80−82] and RI_2•I[17] complexes. Absorption of CH_2I_2•I complexes in the neat solvent CH_2I_2 can be predicted to be reasonably close ($\sim$450 nm) on the basis of correlation between location of absorption and solvent ionization potential.[52] The two-band structure of CT interaction between I• and alkyl iodides is known.[82]

From the transient absorption data of Figures 3−5 and 8a, it can be argued that the CH_2I-I isomer decays via a complex mechanism. Its complete unraveling is beyond the scope of this article, especially when it concerns the reactions among isomer decay products. Nevertheless, several conclusions are reached with regard to the reactions taking place

$$CH_2I-I \rightarrow CH_2I_2 \quad (4)$$

$$CH_2I-I \rightarrow CH_2I\cdot + I\cdot \quad (5)$$

$$CH_2I-I + I\cdot \rightarrow CH_2I_2\cdot I \quad (6)$$

$$CH_2I-I + I\cdot \rightarrow CH_2I_2 + I\cdot \quad (7)$$

$$CH_2I-I + CH_2I\cdot \rightarrow CH_2I\cdot + CH_2I_2 \quad (8)$$

$$2CH_2I-I \rightarrow \text{products} \quad (9)$$

$$CH_2I\cdot + I\cdot \rightarrow CH_2I-I \quad (10)$$

$$CH_2I_2 + I\cdot \rightarrow CH_2I_2\cdot I \quad (11)$$

$$CH_2I_2\cdot I \rightarrow \text{products} \quad (12)$$

$$CH_2I_2\cdot I + ? \rightarrow \text{products} \quad (13)$$

$$2I\cdot \rightarrow I_2 \quad (14)$$

$$2CH_2I\cdot \rightarrow CH_2ICH_2I \quad (15)$$

$$CH_2I\cdot + I\cdot \rightarrow CH_2I_2 \quad (16)$$

From the fitting function type (Figure 8a), it can be concluded that the isomer decays both intramolecularly (eqs 4 and 5) and bimolecularly (eqs 6−9). The square root dependence on the initial isomer concentration (i.e., $[CH_2I-I]$) indicates that the bimolecular part of the decay scheme consists of more than one elementary reaction. This is also concluded from the observed second-order rates (2.55×10^{10} M^{-1} s^{-1}) at the highest $[CH_2I-I]$ in Figure 8a, which are too high to be achieved from only, for example, the isomers reacting with themselves (eq 9). The remaining $1 - \Phi_i \sim 25\%$ fraction of the photofragments, which did not form CH_2I-I, could either exit the cage or recombine into CH_2I_2. The need for isomer reaction partners that are produced photochemically strongly indicates that a majority of the remaining CH_2I• and I• photofragments escapes to participate as catalysts/reactants in the isomer decay (eqs 6−8) on a microsecond time scale. Singular-value decomposition (SVD) analysis of the transient spectra of photolyzed CH_2I_2 (9.3 mM) between 0 and 50 μs shows that at least three distinct spectral components are present. At zero time, the first component consists of the CH_2I-I, CH_2I•, and I• (*n*-C_6H_{14}•I) spectra. At 50 μs, only I_2 is identified clearly. The spectral component between is assigned to an intermediate, which is formed during the isomer decay and decays ultimately forming I_2. The isomer decay rate and the yield of the intermediate both increase on co-photolysis of I_2 indicating that CH_2I-I and I• react to form this intermediate. The formation of I_2 is slower than the bimolecular reaction of iodine atoms leading to I_2 indicating that the intermediate is a relatively stable precursor to I_2. This, in combination with its spectrum, identifies the intermediate as CH_2I_2•I. The overall observed quantum yield of I_2 (moles I_2 formed/moles CH_2I_2 photolyzed) varies from about 10% at $[CH_2I_2] \leq 1$ mM to almost 50% at $[CH_2I_2] = 9.3$ mM indicating that CH_2I_2 is possibly involved in the I_2 formation (eq 11). The reaction 5 presumably dominates over 4 because the radicals produced in eq 5 can react with CH_2I-I via eqs 6−8, in agreement with ab initio predictions that eq 4 is strongly uphill, Figure 7. CH_2I-I decays predominantly intramolecularly (eq 5) at low $[CH_2I-I]$. Direct formation of I_2 from CH_2I-I constitutes, at best, only a minor decay channel. The bimolecular decay routes of CH_2I-I (eqs 6−9), probably being diffusion-controlled, dominate at a high $[CH_2I-I]$. From the CH_2I_2•I yield and that eqs 8 and 9 are competing with eq 6, it can be argued that 6 is more important than 7. CH_2I_2•I decays, possibly, in a second-order fashion (eq 13), in which I_2 is formed either directly or through I•. Gas-phase enthalpies of formation (ΔH_f°)[61,68] indicate that the decomposition of CH_2I_2•I to form I_2 (eq 12) is endothermic and therefore unlikely. The residual radicals presumably disappear via eqs 14,[83] 15,[46] and 16.

3.6.2. Acetonitrile, Methanol, and Ethanol. In acetonitrile (Figure 8b), the k_{obs} rates plotted vs $[CH_2I-I]$ could be fitted to a linear function $k + k_2 \times [CH_2I-I]$ with $k_2 = (4.6 \pm 0.2)$

$\times 10^{10}$ M^{-1} s^{-1} and $k = (4.3 \pm 0.3) \times 10^6$ s^{-1} (230 ± 20 ns lifetime). The ~250 nm band develops with a rise time matching the decay time of CH_2I-I (Figure 4f). This band cannot be attributed to recovery of CH_2I_2 or formation of $I^\bullet$ and $CH_2I^\bullet$ (this radical is observed following the isomer decay, and it absorbs at ~350 nm, like in *n*-hexane) because of their low ϵ and the lack of O_2 effect. Instead, it is assigned to I^- because a charge-transfer-to-solvent absorption of this ion in CH_3CN[53] is the same. Narrow absorption of I^- replaces a broad 220−250 nm band formed during the photolysis pulse (the 0−10 ns spectra, Figures 2 and 4a), with an amplitude that rules out a high degree of participation of $CH_2I^\bullet$ and $I^\bullet$, and hence, attributed to CH_2I-I (ϵ ~2500 M^{-1} cm^{-1} at 250 nm is estimated). This agrees with calculations[60] and reported absorption of the isomer at 254 nm in matrices.[26] From the ϵ(250 nm) values of CH_2I-I and I^- ($\epsilon \sim 12125$ M^{-1} cm^{-1} [53]) and the 5-ns and 75-ns spectra, we calculated that four decaying CH_2I-I species produce about one I^- for the conditions of Figure 4. Absorption of I^- decays as that of I_2^- and I_3^- develops. Under the experimental conditions of Figure 4, minor amounts of I_2^- and I_3^- appear at ~75 ns as traced by absorption of these ions at 750 and 290 nm, i.e., slower than the decay time of CH_2I-I (45 ns). In methanol and ethanol, the decay rates of CH_2I-I were determined to be $(2.0 \pm 0.5) \times 10^8$ s^{-1} and $(1.35 \pm 0.3) \times 10^8$ s^{-1} (Table 1 and Figure 5, inset). The decay is a clean (pseudo) first-order process and not due to reactions with any of the photolysis products because the diffusion-controlled rates would lie at $<10^7$ s^{-1}.[56] Bleaching of CH_2I_2 absorption shows no recovery when CH_2I-I decays (the 0−20 ns spectra in CH_3OH (Figure 5) and the 10−40 ns spectra in C_2H_5OH, not shown), implying that the conversion of CH_2I-I to $CH_2I^\bullet$ and $I^\bullet$ (and, thereafter into CH_2I_2) is not as effective as in other solvents. For $t > 200$ ns in all three solvents, the transient spectra (for $\lambda > 270$ nm) can be accurately fitted to absorption of I_2^- and I_3^-.[84] I_2^- grows to ~200−500 ns and slowly decays with the build up of I_3^-. The 50 μs spectra show ~1:1 amounts of I_2^- and I_3^- in the alcohols and ~1/4 in acetonitrile. Assuming that all I^- ions are trapped into I_3^- and I_2^- at 50 μs and counting the I_3^- and I_2^- absorption, the yield of I^- can be estimated to be 16−23% (Table 2), so the produced amount of I^- in CH_3CN is estimated to ~25% of that of CH_2I-I formed photolytically, consistent with the estimate from the 5 and 75 ns spectra.

We now turn to the reaction mechanism. We have proposed that ionic pathways after breaking of the C−I bond in CH_2I_2 are unlikely before the CH_2I-I product is formed (see section 3.5). Ground-state CH_2I-I may decompose via heterolysis (with ion solvation) to $CH_2I^+ + I^-$ and homolysis to $CH_2I^\bullet + I^\bullet$ from an energy perspective. Homolysis of CH_2I-I followed by electron transfer (concerted with solvation of the incipient ions) seems unlikely because a radical pathway is operative after photohomolysis of CH_2I_2. Therefore, we conclude that I^- is formed directly from CH_2I-I by dissociation of the I−I bond, eq 17

$$CH_2I-I \rightarrow CH_2I^+ + I^- \qquad (17)$$

Loss of I^- liberates the α-iodo-cation, CH_2I^+, the occurrence of which in the photolyzed solutions of CH_2I_2 in CH_3CN was concluded earlier.[14,20] About 1/4 of the isomers produced photolytically form I^-, and the amount of I_3^- and I_2^- formed at 50 μs is the same, indicating that there is no net ion formation after the isomer has decayed. This, combined with heterolysis of CH_2I-I (eq 17), sheds doubt on whether the previously proposed electron transfer within the formed radical pair[14,17] acts in the photochemistry of 1,*n*-diiodoalkanes that can form isomers analogues to CH_2I-I. The isomer lifetime in acetonitrile at low $[CH_2I-I]$ is a factor of ~25 shorter than that in *n*-hexane, which is probably due to the ability of polar solvents to stabilize ionic resonance forms ($H_2C^+-I\cdots I^-$, $H_2C{=}I^+\cdots I^-$, and $H_2C^+-I^--I$) that would more readily undergo both homolytic and heterolytic cleavage of the I−I bond, eqs 5 and 17. The second-order rate of the isomer decay in CH_3CN (4.6×10^{10} M^{-1} s^{-1}) suggests the occurrence of diffusion-controlled reactions with several quenchers. Hence, most of the $CH_2I^\bullet$ and $I^\bullet$ photofragments remaining from combination into CH_2I-I escape the solvent cage in acetonitrile, as in *n*-hexane. Even though eqs 6−9 have some importance in polar solvents (possibly with different products), the reactions between the isomer and its product ions (eqs 18 and 19) are very plausible

$$CH_2I-I + I^- \rightarrow \text{products} \qquad (18)$$

$$CH_2I-I + CH_2I^+ \rightarrow \text{product} \qquad (19)$$

Interestingly, the decay rates of CH_2I-I in methanol and ethanol (2.0 and 1.3×10^8 s^{-1}) are significantly faster than in other solvents. One explanation is a destabilization of CH_2I-I through specific solvation (eq 17). One further possibility is the interaction between the isomer and the OH moiety, e.g., nucleophilic trapping of carbon by the solvent resulting in ether formation.[86] If this occurs, the difference in the above decay rates is expected to correspond to that in the solvent concentrations (17.1 and 26.5 M for C_2H_5OH and CH_3OH, respectively), which is the case within the error limits. Comparable structures, carbene iodine adducts, were stable in dipolar solvents but underwent ionic dissociation in protic solvents.[87] Finally, as time proceeds, the products of the isomer decay react forming stable species, among which only tri-iodide ions are observed spectroscopically in all three solvents. I^- decays as I_2^- and I_3^- are formed and I_2^- is observed as a precursor of I_3^-, indicating the occurrence of eqs 20 and 21, very possibly accompanied by the competing dark reactions 22 and 23,[52] with I_2 being produced in eq 14

$$I^\bullet + I^- \leftrightarrow I_2^- \qquad (20)$$

$$I_2^- + I^\bullet \leftrightarrow I_3^- \qquad (21)$$

$$I_2 + I^- \leftrightarrow I_3^- \qquad (22)$$

$$I_2^- + I_2^- \leftrightarrow I_3^- + I^- \qquad (23)$$

3.6.3. CH_2I_2 versus Other Di- and Polyhalomethanes. The reaction routes following photolysis of CH_2I_2 in polar and nonpolar solvents are summarized in Scheme 1, which can be considered as general for the liquid-phase photochemistry of di- and polyhalomethanes. The CH_2Cl-I and CH_2Br-I isomers of CH_2ClI and CH_2BrI, earlier discovered in matrices,[26,27] are considerably shorter-lived and formed in smaller quantum yields (0.12 and ~2 ns, ~10 and 25%, respectively)[38,59,88] than CH_2I-I ($\lambda_{exc} = 266$ nm, CH_3CN as a solvent). The CHI_2-I isomer of CHI_3 is produced in ~50% yield on 350-nm excitation.[89] Its lifetime is ~1.8 μs in cyclohexane and shorter in acetonitrile (~0.2 μs), a trend also found for CH_2I-I. Isomers as precursors of I^- would easily account for observations of I_3^- when acetonitrile solutions containing CH_2ClI, CH_2BrI, or CHI_3 were photolyzed[59,89] or when trace amounts of ethanol were added to the warmed hydrocarbon glasses of CH_2I_2 and CHI_3 following their exposure to UV light.[90]

SCHEME 1

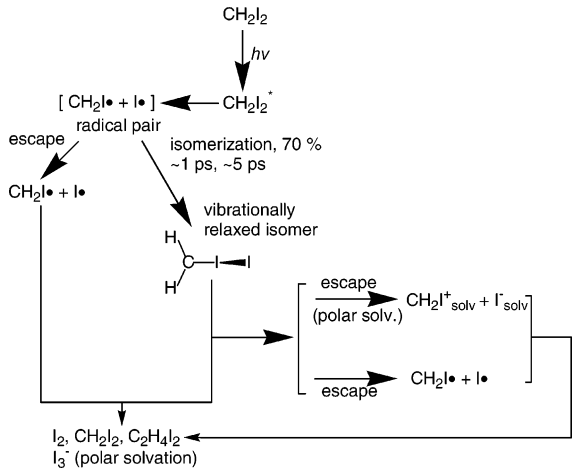

3.7. Quenching of CH_2I-I by Reaction with C=C. Photocyclopropanation. For samples of CH_2I_2 (1 mM) in dichloromethane and acetonitrile, the decay of the CH_2I-I isomer can be accelerated considerably by the addition of cyclohexene, indicating the occurrence of reaction between CH_2I-I and cyclohexene. The addition of cyclohexene to samples of CH_2I_2 in *n*-hexane causes only a somewhat faster decay of CH_2I-I as compared with no addition. A rise of I_2 absorption with the same rate constant as that of the decay of CH_2I-I is observed in the presence of cyclohexene in all three solvents indicating that the iodine molecule product is likely not due to combination of iodine atoms but is generated in the reaction of CH_2I-I with cyclohexene. These results, in conjunction with previous synthetic photochemical studies that identified cyclopropanated products of olefins and I_2 following irradiation of CH_2I_2 with UV light[18−20] and previous DFT computations that indicate CH_2I-I can react with an olefin (ethylene) to produce a cyclopropanated product and I_2 leaving group,[30,31] let us conclude that the observed reaction of CH_2I-I with cyclohexene leads to a photocyclopropanation of the cyclohexene double bond (the norcarane product[18]) and an I_2 leaving group, eq 24

$$CH_2I-I + \text{cyclohexene} \rightarrow \text{norcarane} + I_2 \qquad (24)$$

The observed isomer decay rate in the presence of cyclohexene ($k_{obs-hexene}$) is described by $k_{obs-hexene} = k_{obs} + k_q \times$ [cyclohexene], where k_{obs} is the observed isomer decay rate under the same conditions with no cyclohexene present (Figure 9). The determined second-order rate constants (k_q) at $\lambda = 390$ and 560 nm are similar and lie in the $(4-40) \times 10^5$ M^{-1} s^{-1} range (Table 3). These experiments were mainly performed using 310-nm photolysis light because cyclohexene absorbs strongly at 266 nm (cf. ref 35). The experiment performed in *n*-hexane−cyclohexene mixtures upon excitation at 266 nm gave the k_q rate similar to that determined at $\lambda_{exc} = 310$ nm. After femtosecond excitation of CH_2I_2 (55 mM) in *n*-hexane at 310 nm, the temporal evolution of the 390 nm isomer band on a 100 ps time scale was unaffected by the presence of cyclohexene (0.1, 1, and 2.45 M) within the error limits.

The observed quenching and its time domain is a direct experimental proof that the vibrationally relaxed CH_2I-I isomer reacts with cyclohexene. The determined second-order rate constants of this reaction are smaller than diffusion-limited rates, consistent with the computational results that photocyclopropanation is controlled by a potential barrier.[30,31] We find that the k_q rates increase significantly upon going from *n*-C_6H_{14} to CH_2Cl_2 and CH_3CN, Table 3. We assign this behavior to an increase of relative weights of the "carbenium ion" containing resonance forms ($H_2C^+-I\cdots I^-$ and $H_2C^+-I^--I$) in ground-state CH_2I-I with increased solvent polarity. This would make the carbon atom of CH_2I-I more electrophilic affecting a chemical reactivity of this isomer toward olefin. The relative strength of the visible "iodide-to-carbenium" CT transition with respect to the ~390 nm transition, taken as a measure of the degree of electrophilic character of the isomer carbon, correlates nicely with the k_q rate constants in the solvents *n*-C_6H_{14}, CH_2Cl_2, and CH_3CN, Figure 10.

Thus, the effects of solvent[18] and olefin concentration[20] on quantum yields of the photocyclopropanation reactions that use CH_2I_2 as a reagent can now be readily explained. The yield in a particular solvent is determined by the solvent-specific intramolecular decay of the isomer and the speed of the isomer−olefin reaction (favored by the moderately polar and polar solvents), along with competing trapping of the isomer by radicals in eq 7 and 8 at a relatively high photolysis flux. We

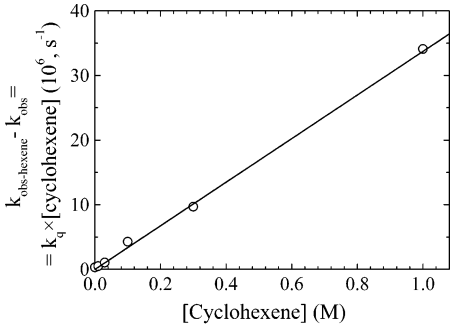

Figure 9. Dependence of the pseudo first-order decay rates of CH_2I-I on cyclohexene content of the photolyzed (0.075 mJ $pulse^{-1}$) sample of CH_2I_2 (1 mM) in deoxygenated CH_2Cl_2. The $k_q = (3.4 \pm 0.2) \times 10^6$ M^{-1} s^{-1} is given by the slope of the linear fit.

TABLE 3: Second-Order Rate Constants (k_q) for the Reaction of CH_2I-I with Cyclohexene[a]

	rate constants (M^{-1} s^{-1})	
solvent	266 nm[b]	310 nm[b]
n-C_6H_{14}	$(4.5 \pm 0.3) \times 10^5$[c]	$(4.4 \pm 0.3) \times 10^5$
CH_2Cl_2		$(3.4 \pm 0.2) \times 10^6$
CH_3CN		$(4.2 \pm 0.9) \times 10^6$

[a] Investigated concentration range of cyclohexene 0.005−1 M. [b] Excitation wavelength. [c] Cyclohexene absorbs strongly at 266 nm on the 1 cm path length and concentrations bigger than 100 mM could not be employed.

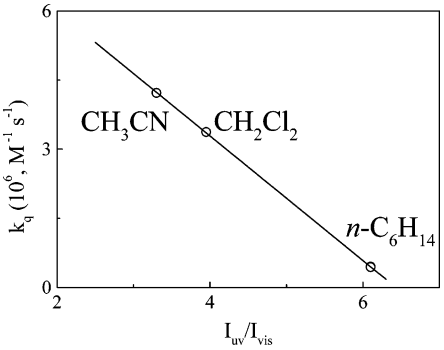

Figure 10. Second-order rate constants for the cyclopropanation reaction between the CH_2I-I isomer and cyclohexene in the solvents CH_3CN, *n*-C_6H_{14}, and CH_2Cl_2 plotted versus the ratio between the amplitudes of the UV band (~390 nm) and the visible CT band (~560−570 nm) of CH_2I-I measured in the same solvents.

SCHEME 2

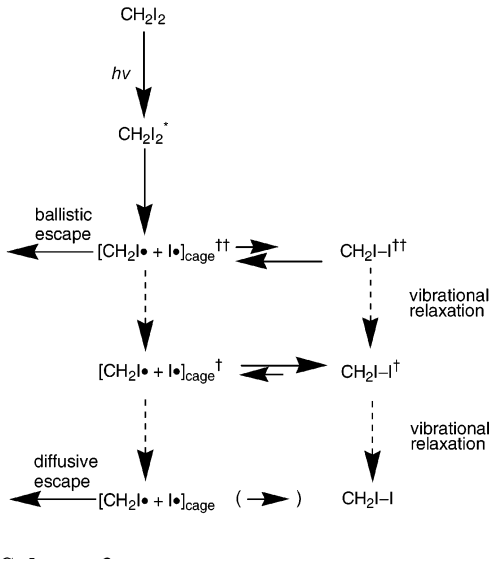

note that small, varying amounts of other addition products to the olefin C=C bond were observed in previous synthetic studies,[18,20] which may have appeared from competing reactions of olefins with photolysis products other than CH_2I-I (e.g., $CH_2I^{\bullet}$). These reactions, to a small degree, may also affects the photocyclopropanation yields.

3.8. Implications of CH_2I-I Stability on the Isomerization Mechanism. CH_2I-I decomposes most easily by direct loss of an iodine atom, i.e., via eq 5, with the rate constant 1.8×10^5 s^{-1} in *n*-hexane. This rate, combined with the assumed Arrhenius preexponential factor of 6×10^{12} s^{-1} (k_BT/h), gives an activation energy of ~42 kJ mol^{-1}, which agrees with the measured apparent activation energy (41 ± 2 kJ mol^{-1}) for this reaction. For thermally activated barrier crossing in solution, the activation energy (E_a) can be empirically expressed as

$$E_a = E_0 + \alpha E_\eta \qquad (25)$$

where E_0 is the barrier height related only with intramolecular properties, E_η is the activation energy of solvent viscosity, and $\alpha \sim 0.3$.[91] The viscosity of *n*-hexane in the 0−50 °C range,[61] fitted to an Arrhenius-like plot, $\eta(T)^{-1} = \eta_0{}^{-1} \exp(-E_\eta/k_BT)$, yields $E_\eta \approx 6.3$ kJ mol^{-1}. Then, $\alpha E_\eta \sim 1.9$ kJ mol^{-1}, and the decomposition energy is estimated to be $E_0 \sim 39$ kJ mol^{-1}. Because of the decay rate of CH_2I-I, a similar threshold energy is likely in the solvent CH_2Cl_2 whereas it is ~8 kJ mol^{-1} smaller in the solvent CH_3CN.

Based on the above thermodynamic estimates and the product translational energy distribution from dissociation of CH_2I_2 in gas phase at 266 nm,[4] the following formation mechanism of the CH_2I-I isomer is proposed, Scheme 2 (the dagger indicates energetically activated molecules). The photoexcited CH_2I_2 molecule dissociates to a highly internally excited $CH_2I^{\bullet}$ radical and an $I^{\bullet}$ atom, with the total energy of the nascent photofragments ~240 kJ mol^{-1}. About 90% of the photofragments were reported to be spread in the translational energy range ~4.2−65 kJ mol^{-1}, with the average energy being ~31 kJ mol^{-1}.[4] As a consequence, a significant amount of vibrational excitation of the I−I bond stretch could be anticipated after the isomers are born. CH_2I-I can house ~220−290 kJ mol^{-1} of the average excess vibrational energy in a harmonic model as calculated from the vibrational frequencies of Zheng and Phillips[32] and using the threshold energy of 31−39 kJ mol^{-1}. This may account for a part of the isomers formed during the first picosecond, provided that their excess vibrational energy is distributed statistically. Energy in excess of 31−39 kJ mol^{-1} initially deposited in the I−I bond stretch will be sufficient to dissociate the isomer. During intramolecular energy redistribution (IVR), the energy leak from the I−I stretch vibration to other isomer normal modes and the energy equilibration will lead to a less efficient dissociation of the isomer. Based on the similar size and number of atoms, IVR in CH_2I-I may be expected to occur on the same time scale as in CH_2I_2, for which the characteristic relaxation times have been shown to be ~10 and 20 ps for the deposited energy of ~72 and 48 kJ mol^{-1}, respectively.[92] The energy removal from "hot" $CH_2I^{\bullet}$ to the solvent could be similarly fast because vibration-to-vibration energy transfer is possible,[5] and thus, this is another way to achieve the stable isomer product. Therefore, the in-cage isomerization of CH_2I_2 to CH_2I-I could be interpreted as "an equilibrium" between the "hot" isomer and radical that shifts toward the isomer as the energy excess in its I−I bond stretch vibration decreases. The time-dependent shift and narrowing of the isomer bands, which is indicative of the change of degree and character of vibrational excitation in CH_2I-I, do occur on the same time scale of several picoseconds as that of the slow CH_2I-I formation. Upon completion of IVR and dissipation of some excess energy to the solvent (~15 ps), the largely equilibrated $CH_2I-I^{\ddagger}$ isomer is attained, which relaxes toward a room-temperature Boltzmann distribution as indicated by the several tens of picoseconds narrowing of the ~390 and ~560 nm bands. The vibrationally cold isomer can survive for microseconds before it statistically dissociates.

Photolysis of CH_2I_2 leads to the CH_2I-I isomer as the main photoproduct. The long-time reactions of CH_2I-I suggest that some $CH_2I^{\bullet}$ and $I^{\bullet}$ photofragments, which do not recombine into this isomer, escape the solvent cage. This most likely happens in a ballistic fashion because of the asymmetry of the product translational energy distribution of Kroger et al.[4] toward high energies. Indeed, the $1 - \Phi_i$ values in this work increase with decreased solvent mass as if cage molecules were more easily pushed aside by the recoiling I atom. Photodissociation studies of OClO and I_2^- have demonstrated that cage escape occurs in ethanol and acetonitrile.[93] Interestingly, we find that geminate reformation of CH_2I_2 does not occur to any appreciable extent. The possible reasons are as follows: (a) Generated by the recoiling I atom, rotation of $CH_2I^{\bullet}$ around its nearly iodine center-of-mass misaligns the radical carbon and iodine fragment reactive sites. The C/I cone of acceptance is narrow because of the bulky iodine of $CH_2I^{\bullet}$. Rotational excitation of the $CN^{\bullet}$ fragment that helps the $ICN \xrightarrow{h\nu} INC$ isomerization is well-known.[94] (b) Time-dependent steric considerations exist for

SCHEME 3

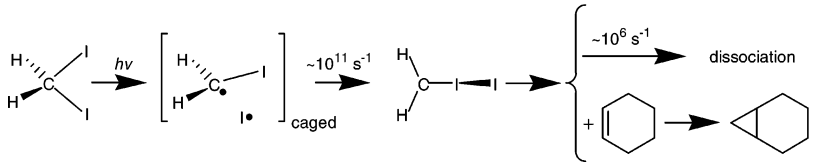

$CH_2I^{\bullet}$. The "incipient" structure of the $CH_2I^{\bullet}$ photofragment is pyramidal with sp^3 hybridization of carbon, whereas the equilibrium structure of $CH_2I^{\bullet}$ is planar with sp^2 bonding of the C atom.[74,95] In the latter structure, an effective electron donation from the $5p_z$ lone pair of iodine to the $2p_z$ unpaired electron on carbon occurs,[96] making the radical iodine chemically reactive. Molecular dynamics investigations of the CH_2I_2 photodissociation in solution should be of great interest.

4. Conclusions

The main findings of this work are summarized in Scheme 3. The CH_2I-I isomer can provide an interesting testing ground for theories of intramolecular vibrational redistribution and solute−solvent interactions in loosely bonded molecules. The efficient trapping of the nascent $CH_2I^{\bullet}$ and $I^{\bullet}$ photofragments in the isomer ground state is achieved within ~15 ps after photohomolysis of CH_2I_2 as a result of vibrational relaxation of "hot" CH_2I-I and $CH_2I^{\bullet}$ because the energy needed to break the isomer I−I bond is measured to only ~31−39 kJ mol^{-1}. Although CH_2I-I can survive out to several microseconds before it dissociates into the radicals and ions, for nonalcoholic solvents, this isomer generally decays faster because it reacts with primary and secondary $CH_2I^{\bullet}$ and $I^{\bullet}$ radicals. In the case of alcoholic solvents, even faster decay of CH_2I-I occurs, likely due to reaction with the solvent. The spectroscopically observed stable products of photolysis of CH_2I_2 are I_2 in nonpolar and moderately polar solvents and I_3^- in polar solvents. We believe that the reaction of photoexcited CH_2I_2 can serve as a model for the corresponding reactions of CRR′XI (R, R′ = side groups, X = Cl, Br, I). The vibrationally relaxed CH_2I-I isomer reacts with cyclohexene added to the solvent leading to an I_2 leaving group, consistent with being the methylene transfer agent in the photocyclopropanation reaction. This result has a general implication for chemical reactivity of CH_2I-I toward carbon double bond, for example, for all cyclopropanation reactions of other olefins that use CH_2I_2 irradiated by UV light as a reagent. The second-order rate constants of the reaction between CH_2I-I and cyclohexene increase with solvent polarity which together with the rate/isomer-CT-absorption correlation highlights the significance of the contact "carbenium-iodide" ion pair resonance structures of the isomer for the photocyclopropanation.

Acknowledgment. We thank B. Nelander, M. Gustafsson, R. Lindh, R. D. Bach, and R. M Hochstrasser for valuable discussions. R. Lindh is also acknowledged for providing the results of his calculations. We are grateful to R. A. L. Smith for careful reading of the manuscript. This research was supported by the Swedish Science Research Council, Magnus Bergwall Foundation, Crafoord Foundation, and Knut and Alice Wallenberg Foundation.

Supporting Information Available: The tables with a summary of spectral assignments made in the literature regarding the UV and visible absorption bands of the photoproduct of CH_2I_2, and with absorption data for the iodine neutral and charged species relevant to the photochemistry of CH_2I_2. This material is available free of charge via the Internet at http://pubs.acs.org.

References and Notes

(1) Rabinowitch, E.; Wood, W. C. *Trans. Faraday. Soc.* **1936**, *32*, 1381. Harris, A. L.; Brown, J. K.; Harris, C. B. *Annu. Rev. Phys. Chem.* **1988**, *39*, 341. Braden, D. A.; Parrack, E. E.; Tyler, D. R. *Coord. Chem. Rev.* **2001**, *211*, 279. Apkarian, V. A.; Schwentner, N. *Chem. Rev.* **1999**, *99*, 1481.

(2) Tarnovsky, A. N.; Alvarez, J.-L.; Yartsev, A. P.; Sundström, V.; Åkesson, E. *Chem. Phys. Lett.* **1999**, *312*, 121.

(3) Kawasaki, M.; Lee, S. J.; Bersohn, R. *J. Chem. Phys.* **1975**, *63*, 809.

(4) Kroger, P. M.; Demou, P. C.; Riley, S. J. *J. Chem. Phys*. **1976**, *65*, 1823.

(5) Baughcum, S. L.; Leone, S. R. *J. Chem. Phys.* **1980**, *72*, 6531.

(6) Schmitt, G.; Comes, F. J. *J. Photochem.* **1980**, *14*, 107. Fotakis, C.; Martin, M.; Donovan, R. J. *J. Chem. Soc., Faraday Trans. 2* **1982**, *78*, 1363. Okabe, H.; Kawasaki, M.; Tanaka, Y. *J. Chem. Phys.* **1980**, *73*, 6162.

(7) Jung, K.-W.; Ahmadi, T. S.; El-Sayed, M. A. *Bull. Korean Chem. Soc.* **1997**, *18*, 1274.

(8) Zhang, J.; Imre, D. G. *J. Chem. Phys.* **1988**, *89*, 309. Zhang, J.; Heller, E. J.; Huber, D.; Imre, D. G.; Tannor, D. *J. Chem. Phys.* **1988**, *89*, 3602.

(9) Marvet, U.; Zhang, Q.; Brown, E. J.; Dantus, M. *J. Chem. Phys.* **1998**, *109*, 4415. Zhang, Q.; Marvet, U.; Dantus, M. *J. Chem. Phys.* **1998**, *109*, 4428.

(10) Williamson, J. C.; Cao, J.; Ihee, H.; Frey, H.; Zewail, A. H. *Nature* **1997**, *386*, 159.

(11) Kwok, W. M.; Phillips, D. L. *J. Chem. Phys*. **1996**, *104*, 2529.

(12) Dantus, M. *Annu. Rev. Phys. Chem.* **2001**, *52*, 639.

(13) Gedanken, A.; Rowe, M. D. *Chem. Phys.* **1979**, *36*, 181.

(14) Kropp, P. J. *Acc. Chem. Res.* **1984**, *17*, 131.

(15) Schwartz, B. J.; King, J. C.; Zhang, J. Z.; Harris, C. B. *Chem. Phys. Lett.* **1993**, *203*, 503. Schwartz, B. J.; King, J. C.; Harris, C. B. In *Ultrafast Dynamics of Chemical Systems*; Simon, J. D., Ed.; Kluwer: Dordrecht, The Netherlands, 1994; pp 235−248.

(16) Saitow, K.; Naitoh, Y.; Tominaga, K.; Yoshihara, K. *Chem. Phys. Lett.* **1996**, *262*, 621.

(17) Miranda, M. A.; Pérez-Prieto, J.; Font-Sanchis, E.; Scaiano J. C. *Acc. Chem. Res.* **2001**, *34*, 717. Miranda, M. A.; Pérez-Prieto, J.; Font-Sanchis, E.; Scaiano J. C. *Prog. React. Kinet. Mech.* **2001**, *26*, 139.

(18) Blomstrom, D. C.; Herbig, K.; Simmons, H. E. *J. Org. Chem*. **1965**, *30*, 959.

(19) Pienta, N. J.; Kropp, P. J. *J. Am. Chem. Soc*. **1978**, *100*, 655.

(20) Kropp, P. J.; Pienta, N. J.; Sawyer, J. A.; Polniaszek, R. P. *Tetrahedron* **1981**, *37*, 3229.

(21) Simons, J. P.; Tatham, P. E. R. *J. Chem. Soc. A* **1966**, 854.

(22) Mohan, H.; Rao, K. N.; Iyer, R. M. *Radiat. Phys. Chem.* **1984**, *23*, 505.

(23) Andrews, L.; Prochaska, F. T.; Ault, B. S. *J. Am. Chem. Soc*. **1979**, *101*, 9.

(24) Mohan, H.; Iyer, R. M. *Radiat. Eff.* **1978**, *39*, 97.

(25) Mohan H.; Moorthy, P. N. *J. Chem. Soc., Perkin Trans. 2* **1990**, *2*, 277.

(26) Maier, G.; Reisenauer, H. P. *Angew. Chem. Int. Ed. Engl.* **1986**, *25*, 819.

(27) Maier, G.; Reisenauer, H. P.; Hu, J.; Schaad L. J.; Hess, B. A., Jr. *J. Am. Chem. Soc.* **1990**, *112*, 5117.

(28) Glukhovtsev, M. N.; Bach, R. D. *Chem. Phys. Lett*. **1997**, *269*, 145.

(29) Orel, A. E.; Kühn, O. *Chem. Phys. Lett.* **1999**, *304*, 285.

(30) Phillips, D. L.; Fang, W.-H.; Zheng, X. *J. Am. Chem. Soc*. **2001**, *123*, 4197.

(31) Phillips, D. L.; Fang, W.-H. *J. Org. Chem*. **2001**, *66*, 5890.

(32) Zheng, X.; Phillips, D. L. *J. Phys. Chem. A* **2000**, *104*, 6880.

(33) Kwok, W. M.; Ma, C.; Parker, A. W.; Phillips, D.; Towrie, M.; Matousek, P.; Phillips, D. L. *J. Chem. Phys.* **2000**, *113*, 7471.

(34) Li, Y.-L.; Wang, D.; Leung, K. H.; Phillips, D. L. *J. Phys. Chem. A* **2002**, *106*, 3463.

(35) Li, Y.-L.; Leung, K. H.; Phillips, D. L. *J. Phys. Chem. A* **2001**, *105*, 10621.

(36) Owrutsky, J. C.; Raftery, D.; Hochstrasser, R. M. *Annu. Rev. Phys. Chem.* **1994**, *45*, 519.

(37) Sukowski, U.; Seilmeier, A.; Elsaesser, T.; Fischer, S. F. *J. Chem. Phys.* **1990**, *93*, 4094. Elsaesser, T.; Kaiser, W. *Annu. Rev. Phys. Chem.* **1991**, *42*, 83.

(38) Tarnovsky, A. N.; Wall, M.; Gustafsson, M.; Lascoux, N.; Sundström, V.; Åkesson, E. *J. Phys. Chem. A* **2002**, *106*, 5999.

(39) Rasmusson, M.; Tarnovsky, A. N.; Åkesson, E.; Sundström, V. *Chem. Phys. Lett.* **2001**, *335*, 201.

(40) Rasmusson, M.; Tarnovsky, A. N.; Pascher, T.; Sundström, V.; Åkesson, E. *J. Phys. Chem. A* **2002**, *106*, 7090.

(41) Åberg, U.; Åkesson, E.; Alvarez, J.-L.; Fedchenia, I.; Sundström, V. *Chem. Phys.* **1994**, *183*, 269.

(42) Pascher, T. *Biochem.* **2001**, *40*, 5812.

(43) Dietz, J.; Merlin, J. *J. Phys. C* **1987**, *48*, 91.

(44) Kimura, K.; Nagakura, S. *Spectrochim. Acta* **1961**, *17*, 166. Ito, M.; Huang, P. C.; Kosower, E. M. *Trans. Faraday Soc.* **1961**, *57*, 1662.
(45) Mössinger, J. C.; Shallcross, D. E.; Cox, R. A. *J. Chem. Soc., Faraday Trans.* **1998**, *94*, 1391. Roehl, C. M.; Burkholder, J. B.; Moortgat, G. K.; Ravishankara, A. R.; Crutzen P. J. *J. Geophys. Res. D* **1997**, *102*, 12819.
(46) Sehested, J.; Ellermann, T.; Nielsen, O. J. *Int. J. Chem. Kinet.* **1994**, *26*, 259.
(47) Bultmann, T.; Ernsting, N. P. *J. Phys. Chem.* **1996**, *100*, 19417.
(48) Kühne, T.; Vöhringer, P. *J. Chem. Phys.* **1996**, *105*, 10788. Kliner, D. A. V.; Alfano, J. C.; Barbara, P. F. *J. Chem. Phys.* **1993**, *98*, 5375. Thomsen, C. L.; Madsen, D.; Thøgersen, J.; Byberg, J. R.; Keiding, S. R. *J. Chem. Phys.* **1999**, *111*, 703. Banin, U.; Ruhman, S. *J. Chem. Phys.* **1993**, *98*, 4391.
(49) Treinin, A.; Hayon, E. *Int. J. Radiat. Phys. Chem.* **1975**, *7*, 387.
(50) Logan, S. R.; Bonneau, R.; Joussot-Dubien, J.; Fornier de Violet, P. *J. Chem. Soc., Faraday Trans. 1* **1975**, *7*, 2148.
(51) Herrmann, V.; Krebs, P. *J. Phys. Chem.* **1995**, *99*, 6794.
(52) Fornier de Violet, P. *Rev. Chem. Interm.* **1981**, *4*, 121.
(53) Jortner, J.; Treinin, A. *Trans. Faraday Soc.* **1962**, *58*, 1503.
(54) Johnson, A. E.; Myers, A. B. *J. Phys. Chem.* **1996**, *100*, 7778.
(55) Fornier de Violet, P.; Bonneau, R.; Joussot-Dubien, J. *Chem. Phys. Lett.* **1973**, *19*, 251.
(56) Product species A and B separated by solvent to a distance l find each other on a time scale t, $t \approx l^2/(D_A + D_B)$, where $D_{A,B}$ are their diffusion coefficients. In the solvent CH_3CN, e.g., $D_I = 4.5 \times 10^{-5}$ cm^2 s^{-1}, $D_{CH_2I} = 3.8 \times 10^{-5}$ cm^2 s^{-1}, and $D_{CH_2I-I} = 3.0 \times 10^{-5}$ cm^2 s^{-1} are based on the Stokes−Einstein equation ($D = \kappa_b T/4\pi\eta r$) with $\eta \approx 0.36$ cP (20 °C), $r_I \approx 2.2$ Å, $r_{CH_2I} \approx 2.35$ Å, $r_{CH_2I-I} \approx 3.0$ Å. Under the conditions of Figures 3−5, ~3% of all CH_2I_2 molecules in the excited volume absorb a photon; therefore, $l \sim 220$ Å for $CH_2I^\bullet$ and $I^\bullet$ products (assuming 30% cage exit), which gives $t \approx 70$ ns. Between CH_2I-I and radicals ($CH_2I^\bullet$ and $I^\bullet$), the l distance is ~180 Å, which yields $t \approx 55$ ns.
(57) Pugliano, N.; Szarka A. Z.; Gnanakaran, S.; Triechel, M.; Hochstrasser, R. M. *J. Chem. Phys.* **1995**, *103*, 6498.
(58) Masaki, A.; Tsunashima, S.; Washida, N. *J. Phys. Chem.* **1995**, *99*, 13126.
(59) Tarnovsky, A. N.; Wall, M.; Rasmusson, M.; Sundström, V.; Åkesson, E. In *Femtochemistry and Femtobiology. Ultrafast Dynamics in Molecular Science*; Douhal, A., Santamaria, J., Eds.; World Scientific: Singapore, 2002; pp 247−260.
(60) Lindh, R. CASPT2/CASSI−SO. For $CH_2I^\bullet$, a strong transition at 271 nm and a weaker at 371 nm are calculated. For CH_2I-I, the computed transitions are at 259, 287, 389, 522, and 856 nm. Unpublished.
(61) *CRC Handbook of Chemistry and Physics*, 80th ed.; Lide, D. R., Ed.; CRC Press LLC: Boca Raton, FL, 1999.
(62) Turner, D. W.; Baker, C.; Baker, A. D.; Brundle, C. R. *Molecular Photoelectron Spectroscopy*; Wiley-Interscience: New York, 1970; p 233.
(63) Bortolini, O.; Hamdan, M.; Traldi, P. *Rapid Comm. Mass Spectrom.* **1992**, *6*, 71.
(64) Mataga, N.; Kubota, T. *Molecular Interactions and Electronic Spectra*; Marcel Dekker: New York, 1970.
(65) Reichardt, C. *Solvents and Solvent Effects in Organic Chemistry*; VCH: Weinheim, Germany, 1988.
(66) Rest, A. J. In *Matrix Isolation Spectroscopy*; NATO Advanced Study Institutes Series, Vol. 76; Barnes, A. J., Orville-Thomas, W. J., Müller, A., Gaufres, R., Eds.; Reidel: Dordrecht, 1980; pp 24−48.
(67) Wintgens, V.; Johnston, L. J.; Scaiano, J. C. *J. Am. Chem. Soc.* **1988**, *110*, 511. Scaiano, J. C.; Barra, M.; Krzywinski, M.; Sinta, R.; Calabrese, G. *J. Am. Chem. Soc.* **1993**, *115*, 8340.
(68) DeCorpo, J. J.; Bafus, D. A.; Franklin, J. L. *J. Chem. Thermodyn.* **1971**, *3*, 125.
(69) Cioslowski, J.; Liu, G.; Moncrieff, D. *J. Am. Chem. Soc.* **1997**, *119*, 9, 11452. Cioslowski, J.; Liu, G.; Moncrieff, D. *J. Phys. Chem. A* **1998**, *102*, 9965.
(70) Marcus, Y. *Ion Solvation*; Wiley: New York, 1985.
(71) Tsai, B. P.; Baer, T.; Werner, A. S.; Lin, S. F. *J. Phys. Chem.* **1975**, *79*, 570.
(72) Chan, D. Y. C.; Mitchell, D. J.; Ninham, B. W. *J. Chem. Phys.* **1979**, *70*, 2946. Chandra A.; Bagchi, B. *J. Phys. Chem.* **1989**, *93*, 6996.
(73) Calculated as $r_s = (3V_{hs}/4\pi)^{1/3}$ using the geometry[74] and hard-sphere volume ($V_{hs} = 47.96$ Å^3) of $CH_2I^\bullet$. V_{hs} was obtained by a correlation scaling[75] the van der Waals volume of $CH_2I^\bullet$ ($V_s = 54.11$ Å^3), which was calculated by means of a technique of overlapping atomic spheres.[76] van der Waals radii of atoms were taken from ref 61.
(74) Kambanis, K. G.; Lazarou, Y. G.; Papagiannakopoulos, P. *Chem. Phys. Lett.* **1997**, *268*, 498.
(75) Ben-Amotz, D.; Herschbach, D. R. *J. Phys. Chem.* **1990**, *94*, 1038.
(76) Meyer, A. Y. *J. Chem. Soc., Perkin Trans. 2* **1985**, *8*, 1161.
(77) The r_v and D values were taken from refs 75 and 61, respectively: 2.122 Å and 35.94 (CH_3CN), 1.918 Å and 32.66 (CH_3OH), and 2.218 Å and 24.55 (C_2H_5OH).
(78) Horng, M. L.; Gardecki, J. A.; Papazyan, A.; Maroncelli, M. *J. Phys. Chem.* **1995**, *99*, 17311.
(79) Hayes, D.; Schmidt, K. H.; Meisel, D. *J. Phys. Chem.* **1989**, *93*, 6100. Schmidt, K. H.; Patel, R.; Meisel, D. *J. Am. Chem. Soc.* **1988**, *110*, 4882.
(80) Shoute, L. C. T.; Neta, P. *J. Phys. Chem.* **1991**, *95*, 4411.
(81) Brühlmann, U.; Büchler, H.; Marchetti, F.; Bühler, R. E. *Chem. Phys. Lett.* **1973**, *21*, 412. Gover, T. A.; Porter, G. *Proc. R. Soc. London Ser. A* **1961**, *262*, 476. Mittal, J. P.; Hamill, W. H. *J. Am. Chem. Soc.* **1967**, *89*, 5749.
(82) Strong, R. L.; Kaye, J. A. *J. Am. Chem. Soc.* **1976**, *98*, 5460.
(83) Marshall, R.; Davidson, N. *J. Chem. Phys.* **1953**, *21*, 2086. Aditya, S.; Willard, J. E. *J. Am. Chem. Soc.* **1957**, *79*, 2680.
(84) By use of the absorption spectrum of I_2^- in methanol[51] with ϵ(387 nm) = 10 700 M^{-1} cm^{-1},[85] and the absorption spectra of I_3^- in acetonitrile or ethanol.[54]
(85) Kühne, T.; Küster, R.; Vöhringer, P. *Chem. Phys.* **1998**, *233*, 161.
(86) Kropp, P. J.; Pienta, N. J. *J. Org. Chem.* **1983**, *48*, 2084.
(87) Kuhn, N.; Kratz, T.; Henkel, G. *J. Chem. Soc. Chem. Commun.* **1993**, 1778. Du Mont, W.-W.; Bätcher, M.; Pohl, S.; Saak, W. *Angew. Chem., Int. Eng. Ed.* **1987**, *26*, 912.
(88) Tarnovsky, A. N.; Wall, M.; Rasmusson, M.; Pascher, T.; Åkesson, E. *J. Chin. Chem. Soc.* **2000**, *47*, 769; Special Issue.
(89) Wall, M.; Tarnovsky, A. N.; Pascher, T.; Sundström V.; Åkesson, E. *J. Phys. Chem. A* **2003**, *107*, 211.
(90) Brown, G. P.; Simons, J. P. *Trans. Faraday Soc.* **1969**, *65*, 3245.
(91) Schroeder J.; Troe, J. In *Activated Barrier Crossing: Applications in Physics, Chemistry and Biology*; Hänggi, P., Fleming, G. R., Eds.; World Scientific: Singapore, 1993, p 206−240.
(92) Charvat, A.; Assmann, J.; Abel, B.; Schwarzer, D.; Henning, K.; Luther, K.; Troe, J. *Phys. Chem. Chem. Phys.* **2001**, *3*, 2230.
(93) Walhout, P. K.; Alfano, J. C.; Thakur, K. A. M.; Barbara, P. F. *J. Phys. Chem.* **1995**, *99*, 7568. Philpott, M. J.; Hayes, S. C.; Reid, P. J. *J. Chem. Phys.* **1998**, *236*, 207.
(94) Krylov, A. I.; Gerber, R. B. *J. Chem. Phys.* **1994**, *100*, 4242. Benjamin, I. *J. Chem. Phys.* **1995**, *103*, 2459. Fernandez-Alberti, S.; Halberstadt, N.; Beswick, J. A.; Echave J. *J. Chem. Phys.* **1998**, *109*, 2844.
(95) Smith, D. W.; Andrews, L. *J. Chem. Phys.* **1973**, *58*, 5222.
(96) Bernardi, F.; Epiotis, N. D.; Cherry, W.; Schlegel, H. B.; Whangbo, M.-H.; Wolfe, S. *J. Am. Chem. Soc.* **1976**, *98*, 469. Yates, B. F.; Bouma, W. J.; Radom, L. *J. Am. Chem. Soc.* **1987**, *109*, 2250. Levchenko, S. V.; Krylov, A. I. *J. Chem. Phys.* **2001**, *115*, 7485.